Biologically Inspired Deadbeat Control of Robotic Leg Prostheses

Ming Pi, Zhijun Li, *Senior Member, IEEE*, Qinjian Li, Zhen Kan, Cuichao Xu, Yu Kang, *Senior Member, IEEE*, Chun-Yi Su, *Senior Member, IEEE*, and Chenguang Yang, *Senior Member, IEEE*

***Abstract*—Recent advances in robotics technology provide great support for robotic leg prostheses to realize full biomechanical functionalities of the contralateral leg. In order to reproduce the biomechanical behaviors of the contralateral leg, this article addresses biologically inspired deadbeat control of robotic leg prostheses under different terrain conditions including level ground, stairs ascent, and descent. The proposed control method is based on the ground reactive force of the contralateral leg during walking. The trajectories of center-of-mass are encoded by the corresponding polynomial splines. Then, the control of the robotic leg prosthesis is designed by replicating the motion of the user's contralateral leg. Compared to most existing results, our approach does not require any preknowledge of the exact physical parameters. Finally, experiments are conducted to show that the prosthesis can help the user walk smoothly under various terrain conditions.**

***Index Terms*—Biologically inspired, deadbeat control, motion imitation, robotic leg prostheses.**

I. Introduction

EVOLVING over millions of years, human walking has gained optimal locomotion for various terrain conditions [1], [2]. Recently, transferring human walking skills to the robotic leg prosthesis attracts growing research interests [3], [4], [27]. However, there are two challenges in controlling the robotic leg prosthesis. The first challenge is how the human walking behaviors can be smoothly adapted to various terrain conditions. The other challenge is how the robotic leg prosthesis can be controlled without complex and empirical preconfigurations.

To address these challenges, many works focused on the redesign of the structure of the robotic leg prosthesis. For lower-limb amputees, the design of robotic leg prostheses in general is either transtibial (below-knee) or transfemoral (above-knee). For instance, in [5], the leg prosthesis was designed to reproduce biomechanical functions of the contralateral leg, with the carbon fiber leaf spring mounted on the ankle and the damping resister on the knee. The passive knee can reproduce the energy cycle process of normal human walking and realize the minimum energy consumption on level ground. For the ankle joint, in [6], the leg prosthesis can reproduce the strike absorption function of the contralateral leg for a number of terrain conditions. The pneumatic structure was introduced for the leg prosthesis to enable the biomechanical function of normal human ankle joint, to realize the heel-strike behavior and the push-off behavior to minimize energy expenditure. For the knee joint, in [7], the damping resister offers the damping resistance for the leg prosthesis to dissipate redundant energy and realizes smooth walking behaviors. Moreover, when incorporating with an electronic control unit, the dampers can emulate various biomechanics of the contralateral leg in various terrain conditions. However, these methods only work well in the preset scenarios and can not adapt to different walking terrain conditions.

Besides the design of the structure of the robotic leg prosthesis, various intelligent controls have been widely used in the works of [8]–[10]. Based on the advances of motor and microelectronic technologies, many novel control methods have been presented (cf., [11] and [12] to name a few). In [13], a mode-specific classification technique was proposed for the control of the robotic leg prosthesis. By collecting and analyzing the data (e.g., the knee and ankle's angle, velocity, and motor current), the mode-specific classifier system was realized to enable smooth transitions between different walking behaviors. Moreover, by investigating the torque-angle curve of the contralateral leg for different walking tasks, the proposed controller can adaptively regulate the impedance characteristics of the leg prosthesis to smoothly switch between walking behaviors and achieve optimal locomotion [14]. With the relationship between

Manuscript received October 27, 2019; revised February 6, 2020 and April 14, 2020; accepted April 19, 2020. Date of publication April 27, 2020; date of current version December 14, 2020. This work was supported in part by the National Natural Science Foundation of China under Grant 61625303, Grant 61751310, and Grant U1913601, in part by the National Key Research and Development Program of China under Grant 2017YFB1302302, Grant 2018YFC2001600, and Grant 2018YFC2001602, and in part by the Anhui Science and Technology Major Program under Grant 17030901029. Recommended by Technical Editor H. A. Varol. *(Corresponding author: Zhijun Li.)*

Ming Pi, Zhijun Li, Qinjian Li, Zhen Kan, and Cuichao Xu are with the Department of Automation, University of Science and Technology of China, Hefei 230027, China (e-mail: piming1987@outlook.com; zjli@ieee.org; lqj0414@mail.ustc.edu.cn; zkan@ustc.edu.cn; xucuichao@126.com).

Yu Kang is with the Department of Automation, Institute of Advanced Technology, University of Science and Technology of China, Hefei 230027, China (e-mail: kangduyu@ustc.edu.cn).

Chun-Yi Su is with the School of Automation, Guangdong University of Technology, Guangzhou 510006, China, and also with the Concordia University, Montreal, QC H3G 1M8, Canada (e-mail: cysu@alcor.concordia.ca).

Chenguang Yang is with the Bristol Robotics Laboratory, University of the West of England, Bristol BS16 1QY, U.K. (e-mail: cyang@ieee.org).

Color versions of one or more of the figures in this article are available online at https://ieeexplore.ieee.org.

Digital Object Identifier 10.1109/TMECH.2020.2990406

the myoelectric signals and the angle and torque of the joints, the change of myoelectric signals was investigated to predict the upcoming mode transitions [15]–[17], which improves the control performance of robotic prostheses in various walking modes. In [18], a learning approach was proposed to regulate the impedance parameters of the leg prosthesis. However, this learning approach was based on the invariant locomotion trajectories observed from unimpaired human walkers. Moreover, the initial parameters need to be tuned experimentally by clinicians. In [19], the method based on fuzzy logic inference was proposed to encode the human walking experience to regulate the control parameters of the leg prosthesis, which reproduces the able-bodied knee's trajectory during walking. However, this method heavily relies on the knowledge of human walking and requires more sensors. In [20], a gain learning control method was proposed to correct the joint's torque of the leg prosthesis to mimic the behavior of the intact limb of subject. However, this method needs the inverse dynamics of the leg prosthesis to estimate the ankle's torque, which limits its use in a laboratory environment.

Despite the advantage of adaptive control, there exists a major challenge in the configuration of the robotic leg prosthesis [21]–[23]. That is, prostheses need more complex preconfigurations and empirical tuning of its control parameters [24], [25]. In [26]–[28], the control parameters have to be tuned individually for different prostheses. However, there does not exist a systematic approach to guide the parameter tuning for different configurations with different prostheses. Hence, it is crucial to find a model-free control approach such that, without complex preconfigurations and empirical tuning of control parameters, the controller can smoothly achieve walking behaviors without exact knowledge of dynamics of leg prostheses among different walking tasks.

It is observed from human walking experiments that the trajectory of human body's center-of-mass (CoM) and the change of leg forces during the stance phase can be encoded by polynomial splines [29]. Inspired by this observation, many results exploited polynomial splines for the control of robotic leg prostheses. However, these studies need complex preconfigurations and empirical tuning of control parameters for the leg prosthesis to perform different walking tasks. In [30], the control strategy was proposed for the leg prothesis, which increased and decreased the joints' stiffness during different walking phases. However, this control strategy has to be predefined for different walking tasks. In [31], the employed control method combined with the impedance-weight-bearing portion's framework for the regulation of trajectory of the leg prosthesis. However, this control method was only proposed for the level ground walking and needs empirical tuning of control parameters of the leg prosthesis. In [32], the prosthesis controller is based on hybrid zero dynamic model and is robust to continuous moderate perturbations with the complex precongurations of the leg prosthesis. In [33], a classifying method has been used to recognize different terrain types. By predefining the initial parameters, the environmental features can be obtained and integrated within the motion control of leg prosthesis.

Aligned with previous researches, we proposed a control method based on polynomial splines to enable smooth transitions among various walking behaviors. Motivated to transfer normal human walking behaviors to the robotic leg prosthesis, our control method can adapt walking behaviors for different terrain conditions without complex preconfigurations and empirical tuning of control parameters of the leg prosthesis.

The contributions of this article include the following. The walking of the leg prosthesis is encoded by polynomial splines using the initial position, the end position, and the time interval between steps, recorded by inertial measurement unit (IMU) mounted on the contralateral leg of subject. The walking trajectories can be reshaped according to different walking tasks, without complex preconfigurations and empirical tuning of the leg prosthesis. The proposed control method can smoothly achieve walking behaviors and diminish the overshoot of input torques caused by the large initial error at the beginning of the transient response, without exact knowledge of dynamics of leg prosthesis among different walking tasks.

II. Human Walking Experiments and Planning Method for Walking Trajectory

As indicated in [29], the trajectories of the CoM can be encoded by the polynomial splines. The ground reactive force (GRF) profile has been recorded during the human-walking experiment on the force plate, as shown in Fig. 1. Without the consideration of the impact phenomenon at the begin of the stance phase and the lower slope at the end, the GRF profile can be formulated as the two-order polynomial in the vertical direction and the three-order polynomial in the horizontal direction. Hence, the leg force profile can be also approximated with polynomials. The total force F_{CoM} on the CoM of subject can be formulated as [29]

$$F_{\mathrm{CoM}} = F_{\mathrm{leg}} + F_g = F_{\mathrm{leg}} + HG \tag{1}$$

where F_{leg} represents the leg force, F_g represents the gravitational force, H represents the robot's mass, and $G = [0, 0, -g]^T$. According to Newton's second law, we can encode the position of the vertical CoM by the polynomials of order 4 and the horizontal position by the polynomials of order 5. The CoM position profiles are presented as [29]

$$\begin{aligned}\begin{bmatrix} u(t) \\ \dot{u}(t) \\ \ddot{u}(t) \end{bmatrix} &= \begin{bmatrix} 1 & t & t^2 & t^3 & t^4 & t^5 \\ 0 & 1 & 2t & 3t^2 & 4t^3 & 5t^4 \\ 0 & 0 & 2 & 6t & 12t^2 & 20t^3 \end{bmatrix} r_u \\ &= \begin{bmatrix} t_u^T(t) \\ t_{\dot{u}}^T(t) \\ t_{\ddot{u}}^T(t) \end{bmatrix} r_u,\ u \in \{x, y, z\} \end{aligned} \tag{2}$$

where $t_u^T(t)$, $t_{\dot{u}}^T(t)$, and $t_{\ddot{u}}^T(t)$ represent the time mapping; r_u represents the polynomial parameters; $u(t)$, $\dot{u}(t)$, and $\ddot{u}(t)$ represent CoM positions, velocities, and accelerations, respectively.

As shown in Fig. 2, the previewed steps of the robotic leg prosthesis during swing and stance phase can be derived according to the boundary conditions mentioned previously. Let v represent the vertical direction, i.e., $v \in \{z\}$. In Fig. 2, v_{TD} represents the height of the trajectory of CoM, v_{floor} represents the height of the level ground, $\Delta v_{TD,\mathrm{des}}$ represents the difference between v_{TD} and v_{floor}, f_1 and f_2 represent the touch-down points,

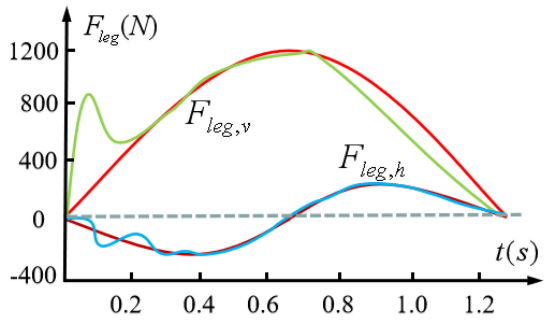

Fig. 1. GRF of the contralateral leg during stance phase.

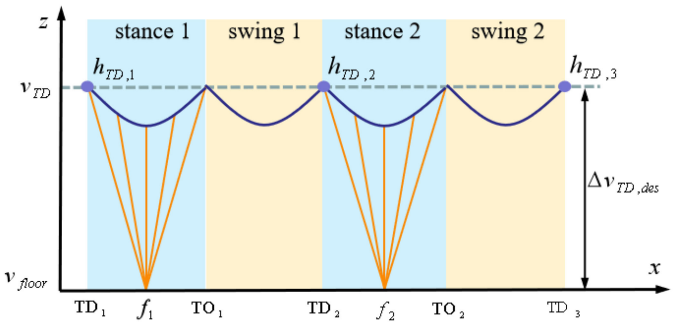

Fig. 2. Previewed steps of the robotic leg prosthesis during swing and stance phases.

$h_{TD,i}, i = 1, 2, 3$ represent the height of start position of step i, $TD_i, i = 1, 2, 3$ represent the heel strike moment of step i, $TO_i, i = 1, 2, 3$ represent the leave off moment of step i, T_s represents the total stance time, and T_w represents the total swing time. For each previewed step, the vertical boundary condition can be yield as [29]

$$\begin{bmatrix} v_{TD,i} \\ \dot{v}_{TD,i} \\ -g \\ -g \end{bmatrix} = \begin{bmatrix} t_{v(0)}^T \\ t_{\dot{v}(0)}^T \\ t_{\ddot{v}}^T(0) \\ t_{\ddot{v}}^T(T_{s,i}) \end{bmatrix} r_{v,i} \tag{3}$$

where i represents the step index; $e_{v,i} = [v_{TD,i}, \dot{v}_{TD,i}, -g, -g]^T$ represents the boundary condition; $E_{v,i} = [t_v^T(0), t_{\dot{v}}^T(0), t_{\ddot{v}}^T(0), t_{\ddot{v}}^T(T_{s,i})]$ represents the mapping of boundary conditions; $r_{v,i}$ represents the parameters of the vertical polynomial. The first element in $e_{v,i}$ represents the CoM position. The second element in $e_{v,i}$ represents the CoM velocity. The other elements represent the accelerations of CoM at the begin and the end of the stance phase, respectively. Then, $E_{v,i} r_{v,i} = e_{v,i}$ is solved as [29]

$$r_{v,i} = E_{v,i}^T (E_{v,i} E_{v,i}^T)^{-1} e_{v,i} + w_{v,i} \tilde{r}_{v,i}. \tag{4}$$

Then, $E_{v,i}$ will be obtained by the scalar variable $\tilde{r}_{v,i}$. For $E_{v,i} w_{v,i} = 0$, we have [29]:

$$w_{v,i} = \begin{bmatrix} -E_{v,i,\text{square}}^{-1} E_{v,i,\text{final}} \\ 1 \end{bmatrix} \tag{5}$$

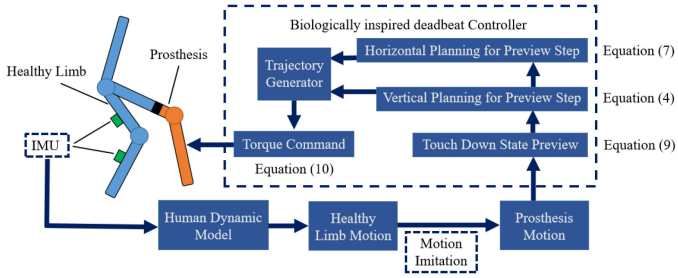

Fig. 3. Diagram of the proposed control method.

where $E_{v,i,\text{final}}$ represents the last column in $E_{v,i}$; $E_{v,i,\text{square}}$ represents all of the other columns.

Let h represent the horizontal direction, i.e., $h \in \{x, y\}$. For the previewed steps, five horizontal boundary conditions are defined as [29]

$$\begin{bmatrix} h_{TD,i} \\ \dot{h}_{TD,i} \\ 0 \\ 0 \\ h_{TD,i+1,des} \end{bmatrix} = \begin{bmatrix} t_h^T(0) \\ t_{\dot{h}}^T(0) \\ t_{\ddot{h}}^T(0) \\ t_{\ddot{h}}^T(T_{s,i}) \\ t_h^T(T_{s,i}) + T_{w,i} t_{\dot{h}}^T(T_{s,i}) \end{bmatrix} r_{h,i} \tag{6}$$

where $e_{h,i} = [h_{TD,i}, \dot{h}_{TD,i}, 0, 0]^T$ represents the horizontal boundary condition; $E_{h,i} = [t_h^T(0), t_{\dot{h}}^T(0), t_{\ddot{h}}^T(0), t_{\ddot{h}}^T(T_{s,i}), t_h^T(T_{s,i}) + T_{w,i} t_{\dot{h}}^T(T_{s,i})]^T$ represents the mapping of boundary conditions; $r_{h,i}$ represents the polynomial parameters. The first element of $e_{h,i}$ represents the initial CoM position. The second element of $e_{h,i}$ represents the initial CoM velocity. The next two elements represent, respectively, the initial and final CoM accelerations. The fifth element denotes the next horizontal step as $h_{TD,i+1,des}$

$$\begin{aligned} h_{TD,i+1,des} &= h_{TO,i} + T_{w,i} \dot{h}_{TO,i} \\ &= (t_{h,i}^T(T_{s,i}) + T_{w,i} t_{\dot{h}}^T(T_{s,i})) r_{h,i}. \end{aligned} \tag{7}$$

Hence, the general solution of (6) will be given by [29]

$$r_{h,i} = E_{h,i}^T (E_{h,i} E_{h,i}^T)^{-1} e_{h,i} + w_{h,i} \tilde{r}_{h,i} \tag{8}$$

where $w_{h,i}$ is computed from (11).

III. Control Method for Robotic Leg Prosthesis

The proposed control method for the leg prosthesis works in a two-level control structure. At the top level, the desired CoM trajectories for each phase are generated for the joint by the above mentioned planning method. At the lower level, the control method conducts the torque control for each joint based on the command from the top level with the designed controller.

In Fig. 3, the motion states collected by IMU are used to reconstruct the contralateral leg motion by the human dynamic model. Then, the proposed control method implements the motion of leg prosthesis to track the motion of the contralateral leg [34]. Then, the vertical and horizontal plannings can be calculated by the abovementioned planning method. Moreover, the desired

CoM trajectory was generated for the torque control of joints of the robotic leg prosthesis. At last, the leg prosthesis behaves the motion of the contralateral leg. Walking steps are switched by the GRF from the prosthesis, which are measured from the force sensor on the prosthesis. The swing phase is switched when the foot leaves the ground and the GRF drops to less than -10 N. To avoid premature transition, the GRF during the stance phase must not exceed -200 N. In addition, a 500 ms time delay ensures the numerical stability of the GRF.

A. Motion Imitation

In normal cases, the motion imitation control is proposed for the preplanning of each step of the robotic leg prosthesis. The motion of the prosthesis aims to replicate the movement of user's contralateral leg in both swing and stance phases under desired boundary conditions. The preplanning of each step of the robotic leg prosthesis is in the form of [29]

$$\begin{bmatrix} u_{TO,1} \\ \dot{u}_{TO,1} \end{bmatrix} = \begin{bmatrix} u \\ \dot{u} \end{bmatrix} + \begin{bmatrix} t_u^T(T_{s,1}) - t_u^T(t_s) \\ t_{\dot{u}}^T(T_{s,1}) - t_{\dot{u}}^T(t_s) \end{bmatrix} r_{u,1}, u \in \{h, v\} \tag{9}$$

where $t_u^T(t)$ and $t_{\dot{u}}^T(t)$ are the same row vectors of time mapping from (2). They can predict how much an offset is desired. This offset is calculated by the motion of user's contralateral leg during the last swing phase. Then, we can predict the next swing phase of the leg prosthesis and compute the upcoming step by compensating the offset to the current phase. The merit of the proposed control is that the heel strike point of next step can be updated according to the desired CoM reference trajectory in real time.

B. Controller Design

The controller of this article is designed for various walking conditions. The controller is designed as

$$\tau = -K_D \Delta\dot{q} - K_P s(\Delta q) \tag{10}$$

where τ is the torque for the joint of the prosthesis, $K_D = \text{diag}[k_{D1}, \ldots, k_{Dn}]$, $k_{D1}, \ldots, k_{Dn} \in \mathbb{R}$, denotes the velocity control gains, $K_P = \text{diag}[k_{P1}, \ldots, k_{Pn}]$, $k_{P1}, \ldots, k_{Pn} \in \mathbb{R}$, denotes the angular control gains, $\Delta q = [\Delta q_1, \ldots, \Delta q_n]^T = q - q_d, s(\Delta q) = [s_1(\Delta q_1), \ldots, s_n(\Delta q_n)]^T$, and $s_1, \ldots, s_n \in \mathbb{R}$ are saturated functions designed as

$$s_i(\Delta q_i) = \begin{cases} 1 & \text{for } \Delta q_i > \frac{\pi}{2} \\ \sin(\Delta q_i) & \text{for } -\frac{\pi}{2} \le \Delta q_i \le \frac{\pi}{2} \\ -1 & \text{for } \Delta q_i < -\frac{\pi}{2}. \end{cases} \tag{11}$$

C. Stability Analysis

The robotic leg prosthesis moves according to the following dynamics:

$$H(q(t))\ddot{q}(t) + \left\{\frac{1}{2}\dot{H}(q(t)) + C(q(t), \dot{q}(t)) + D\right\}\dot{q}(t) + G(q(t)) = \tau(t) \tag{12}$$

where $H(q) \in \mathbb{R}^{n\times n}$ is a positive-definite inertia matrix, $C(q, \dot{q}) \in \mathbb{R}^{n\times n}$ is a skew symmetric matrix, $D = \text{diag}[d_1, \ldots, d_n]$ is a viscosity matrix, $d_1, \ldots, d_n \in \mathbb{R}$, $G(q) \in \mathbb{R}^n$ represents a gravity acceleration, $q = [q_1, \ldots, q_n]^T$ represents the joint angles, $\tau = [\tau_1, \ldots, \tau_n]^T$ represents the actuator torque, and $t \in \mathbb{R}$ is time.

Assuming the positive constants $c_{r\max}$, c_s, and $c_g \in \mathbb{R}$, (12) satisfies the following inequalities. $\lambda_{\max}(H(q)) \le c_{r\max}$. $\|C(q, \dot{q})\| \le c_s\|\dot{q}\|$. $\|G(q)\| \le c_g$. $\lambda_{\max}(H(q))$ denotes the maximum eigenvalue of $H(q)$, and $\|C(q, \dot{q})\|$ represents the matrix norm of $C(q, \dot{q})$, and $\|\dot{q}\|$ represents the Euclidian norm of $\dot{q}$.

Then, the Lyapunov candidate can be chosen for the stability analysis

$$\begin{aligned} V(t) = &\frac{1}{2}\Delta\dot{q}^T H(q)\Delta\dot{q} \\ &+ \Sigma_{i=1}^n((1-c)(k_{Pi} + a_i k_{Di}) + a_i d_i) r_{si}(\Delta q_i) \\ &+ \Delta\dot{q}^T H(q) A s(\Delta q) \end{aligned} \tag{13}$$

where $r_{si}(\Delta q_i) = \int_0^{\Delta q_i} s_i(r)dr$, $r_{si}(0) = 0, (i = 1, 2, \ldots, n)$ represents the potential functions; $c \in \mathbb{R}$ is a positive constant, satisfying $0 \le c < 1$, and $A = \text{diag}[a_1, \ldots, a_n] = K_P K_D^{-1}$.

In (13), we expand the third term as

$$\begin{aligned} &\Delta\dot{q}^T H(q) A s(\Delta q) \\ &= \frac{1}{2}(\Delta\dot{q} + A s(\Delta q))^T H(q)(\Delta\dot{q} + A s(\Delta q)) \\ &\quad - \frac{1}{2}\Delta\dot{q}^T H(q)\Delta\dot{q} - \frac{1}{2}s(\Delta q)^T A^T H(q) A s(\Delta q). \end{aligned} \tag{14}$$

According to (12), the potential functions $r_{si}(\Delta q_i)$ are always greater than $\frac{1}{2}s_i(\Delta q_i)^2$, and the second term in (13) is greater than $\frac{1}{2}\Sigma_{i=1}^n(2(1-c)a_i k_{Di} + a_i d i)s_i(\Delta q_i)^2$. Then, the third term in (14) is greater than $-\frac{1}{2}c_{r\max}\Sigma_{i=1}^n r_i^2 s_i(\Delta q_i)^2$. Then, by choosing $a_i < \frac{2k_{Di}(1-c)+d_i}{c_{r\max}}$, the sum of the two terms is positive. As a result, we can ensure that the function V is positive definite. Hence, we can deduce (13) as

$$\begin{aligned} \dot{V} = &-\Delta\dot{q}^T(K_D + D)\Delta\dot{q} - s(\Delta q)^T A K_P s(\Delta q) \\ &- 2c\Delta\dot{q}^T A k_D s(\Delta q) + \frac{1}{2}\Delta\dot{q}^T\dot{H}(q) A s(\Delta q) \\ &+ \Delta\dot{q}^T H(q) A\dot{s}(\Delta q) + y^T z \end{aligned} \tag{15}$$

and

$$\begin{aligned} z = &-\{H(q) - H(q_d)\}\ddot{q}_d - \frac{1}{2}\{\dot{H}(q) - \dot{H}(q_d)\}\dot{q}_d \\ &- \{s(q, \dot{q}) - s(q_d, \dot{q}_d)\}\dot{q}_d - s(q, \dot{q})\Delta\dot{q} - G(q) + G(q_d). \end{aligned} \tag{16}$$

Therefore, we can have the last three items in (15) as

$$\begin{aligned} &y^T z + \frac{1}{2}\Delta\dot{q}^T\dot{H}(q) A s(\Delta q) + \Delta\dot{q} H(q) A\dot{s}(\Delta q) \\ &\le \|\Delta\dot{q}\|^2_{l_1 I + l_2 A} + \|s(\Delta q)\|^2_{l_3 I + l_4 A + l_5 A^2} \end{aligned}$$

$$l_1 = \left(\frac{1}{2}c_{r\max} + c_s\right) c_{dv}\frac{3+2c_{dv}}{2} + c_{r\max}c_{da} + c_g + \frac{1}{2}c_s c_{dv} + \frac{1}{4}c_{r\max}c_{dv}$$

$$l_2 = c_s + \frac{3}{2}c_{r\max}$$

$$l_3 = \left(\frac{1}{2}c_{r\max} + c_s\right) c_{dv}^2 + c_{r\max}c_{da} + c_g$$

$$l_4 = 2\left(\frac{1}{2}c_{r\max} + c_s\right) c_{dv}^2 + 2c_{r\max}c_{da} + 2c_g$$

$$l_5 = \frac{1}{2}\left(\frac{1}{2}c_{r\max} + c_s\right) c_{dv} + \frac{1}{2}c_s c_{dv} + \frac{1}{4}c_{r\max}c_{dv}. \quad (17)$$

Moreover, $\tau^T F\tau = \Delta\dot{q}^T K_D \Delta\dot{q} + 2\Delta\dot{q}^T A K_D s(\Delta q) + s(\Delta q)^T K_P A s(\Delta q)$. Then, we can have

$$-2c\Delta\dot{q}^T A K_D s(\Delta q) = -c\tau^T F\tau + cs(\Delta q)^T K_P A s(\Delta q) + c\Delta\dot{q}^T K_D \Delta\dot{q}. \quad (18)$$

Finally, we can deduce V as

$$\dot{V} \le -\Delta\dot{q}^T C_D \Delta\dot{q} - s(\Delta q)^T C_P s(\Delta q) - c\tau^T F\tau < 0$$

$$C_D(c) = (1-c)K_D + D - c_1 I - c_2 A$$

$$C_P(c) = (1-c)AK_P - c_3 I - c_4 A - c_5 A^2. \quad (19)$$

Since, $\dot{V}$ is negative, the stability of the system will be ensured.

IV. Experiments and Results

A. Experiments Setup

In this article, four experiments have been conducted to verify the performance of the proposed control method for different walking tasks. The mechanical structure of the robotic leg prosthesis has been shown as Fig. 6. The leg prosthesis owns two powered joints and has been designed by the USTC Robotic Laboratory.

In the experiments, three healthy participants are recruited and agree to participate in the study: subject 1 is 25 years old, 172 cm and 65 kg; subject 2 is 24 years old, 175 cm and 70 kg; subject 3 is 26 years old, 180 cm and 75 kg.

The mechanical structure of the leg prosthesis has been constructed with the aluminum alloy and the nylon fiber. As shown in Table I, the total weight of robotic prosthesis is 4.8 kg, close to a healthy lower limb. As shown in Table II, the flexion of the knee joint is about $120°$. The planterflexion and dorsiflexion of the ankle joint are about $-45°$ and $25°$, respectively. The actuator for the knee joint of the prosthesis is located under the thigh receiving cavity interface. The actuator for the ankle joint is mounted on the back of the prosthesis. By changing the length from the ball nut of footplate to the pyramid connector of knee joint, the length of the leg prosthesis can be adjusted. Data recordings acquired from IMU and Force sensors are used in the analysis during experiments. The Trigno wireless wearable sensors of Delsys Co., Ltd. are mounted on the user's contralateral leg in the experiments, which integrates the IMU sensors. The joints of the prosthesis are driven by Maxon dc flat brushless motor EC45. The servo driver Elmo connects with the computer via a CAN bus, to control the Maxon EC 45 Power Max brushless motors. The interface was designed on the computer to monitor the change of signals of sensors mounted on the leg prosthesis, sampled at 1 kH. Through this interface, the information such as the position, velocity, and torque can be stored and analyzed. The mechanical limit for the joints of the prosthesis can avoid the excessive movement in the experiments.

TABLE I
MASS OF LEG PROSTHESIS

Part name	Mass(kg)	Percentage
Main Part	1.06	22%
Ankle Motor	0.91	19%
Knee Motor	1.01	21%
Servo Driver	0.38	8%
Foot Plate	0.86	18%
Shell	0.58	12%
Total	4.8	100%

TABLE II
CONFIGURATIONS OF LEG PROSTHESIS

Part name	Value
Mass of Prosthesis	4.8 kg
Length of Prosthesis	0.40 m to 0.52 m
Range for Knee	$0°$ to $120°$
Max Torque for Knee	80 Nm
Max Power for Knee	90 W
Range for Ankle	$-45°$ to $25°$
Max Torque for Ankle	100 Nm
Max Power for Ankle	90 W

B. Case S1

1) Experiment: The case is to verify that the control performance of the proposed method is better than the method adopting a preset fixed motion.

2) Results: The subject walks on the level ground with the leg prosthesis. Because of the preset fixed motion, the walking length, and frequency of leg prosthesis cannot be regulated by the subject. Meanwhile, IMU on the contralateral leg provides the real walking length and frequency of the subject. Fig. 7(a) shows that the motion of leg prosthesis is fixed all time. Fig. 7(b) shows that the motion of the contralateral leg is unfixed. The subject with the prosthesis can keep walking and adjusts the walking speed and direction freely. As shown in Fig. 7, the subject can not regulate the motion of leg prosthesis because of the preset fixed motion.

C. Case S2

1) Experiment: This case is to verify that the proposed method has a better performance than the method only replicating the movement of the healthy lower limb.

2) Results: The subject walks on the level ground with the leg prosthesis. The walking length and frequency of leg

Fig. 4. Human-walking experiment on the level ground.

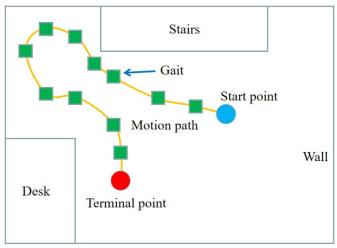

Fig. 5. Motion path on the level ground.

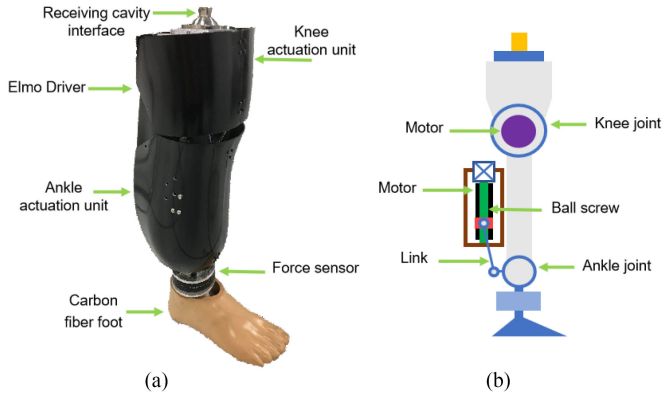

Fig. 6. Mechanical structure of the leg prosthesis.

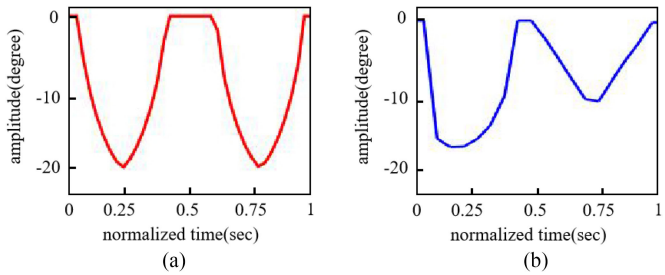

Fig. 7. Change of knee joint in Case S1. (a) Fixed motion of leg prosthesis. (b) Real motion of contralateral leg at the same time.

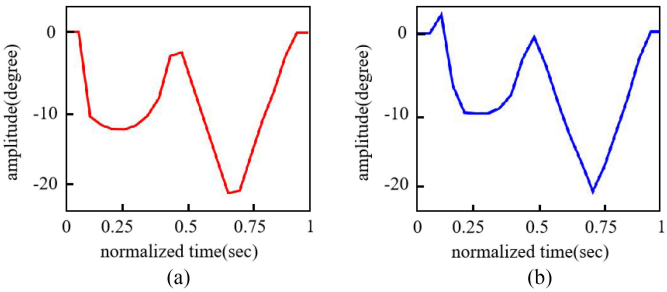

Fig. 8. Change of knee joint in Case S2. (a) Real trajectory of the leg prosthesis' knee joint which imitates the motion of contralateral leg. (b) Desired trajectory of the leg prosthesis' knee joint generated from the proposed method.

prosthesis can be regulated directly by the contralateral leg of subject with the collected joint's value from IMU. Meanwhile, IMU on the contralateral leg provides the real walking length and frequency of the subject. Fig. 8(a) reveals the change of the knee' angle, which replicates the movement of the healthy lower limb. Fig. 8(b) reveals the change of the knee' angle by the proposed method. The subject with the prosthesis can keep walking and adjusts the walking speed and direction freely. As shown in Fig. 8, the subject can regulate the motion of leg prosthesis.

D. Case S3

1) Experiment: This case is to verify the performance of the proposed control method on the level ground. The subject walks on the level ground with the leg prosthesis in Fig. 4. As shown in Fig. 5, the subject walks back and forth between two ends in the room. The walking length and frequency are guided by the contralateral leg. Hence, the subject with the prosthesis can keep walking and adjusts the walking speed and direction freely.

2) Results: The results in this experiment are shown as Figs. 9–12.

The trajectory tracking performance of the three subjects are shown in Figs. 9(a) and (b), 10(a) and (b), and 11(a) and (b). The tracking errors are shown as Figs. 9(c), 10(c), and 11(c). The average deviation for different subjects is shown as Table III. By regulating the parameters of leg prosthesis, the minimized mean square error (MSE) reduces to 0.096 rad, 0.074 rad, and 0.074 rad for subject 1, 2, and 3, respectively. The torque for each joint is shown as Figs. 9(d), 10(d), and 11(d). Fig. 12 shows the GRF during walking, which fits the two order curve as shown in Fig. 1. As shown previously, the tracking errors are small.

TABLE III
TRAJECTORY TRACKING PERFORMANCE OF THREE SUBJECT IN CASE S3

Subject	MEAN(rad)	MSE(rad)
1	0.014	0.060
2	0.010	0.046
3	0.012	0.055

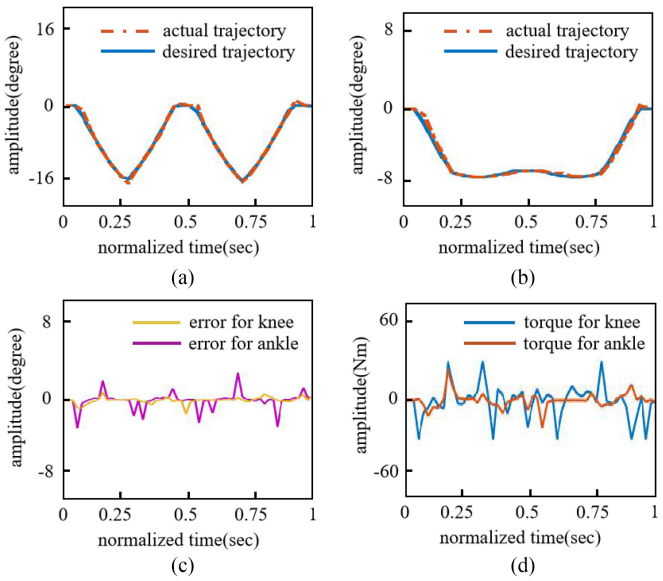

Fig. 9. Experimental results of subject 1. (a) Tracking trajectory of knee joint. (b) Tracking trajectory of ankle joint. (c) Trajectory error. (d) Torque of each joint.

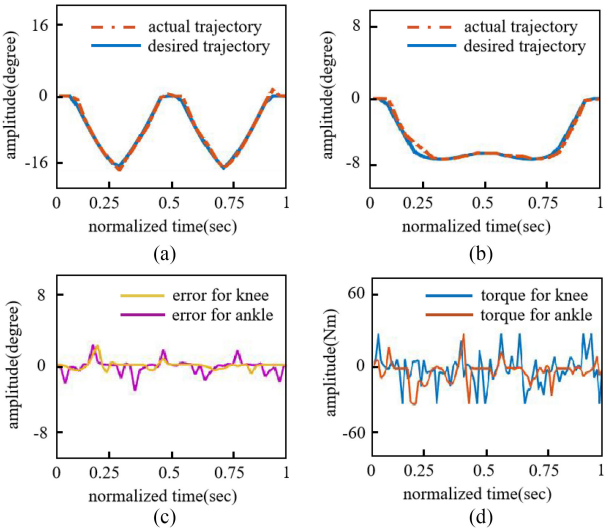

Fig. 10. Experimental results of subject 2. (a) Tracking trajectory of knee joint. (b) Tracking trajectory of ankle joint. (c) Trajectory error. (d) Torque of each joint.

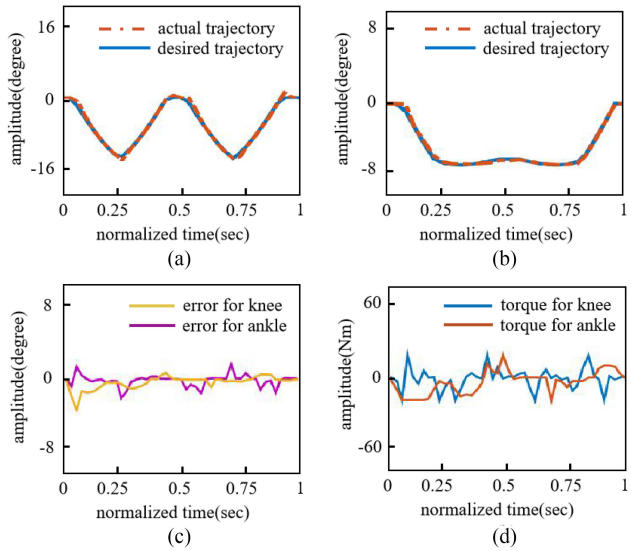

Fig. 11. Experimental results of subject 3. (a) Tracking trajectory of knee joint. (b) Tracking trajectory of ankle joint. (c) Trajectory error. (d) Torque of each joint.

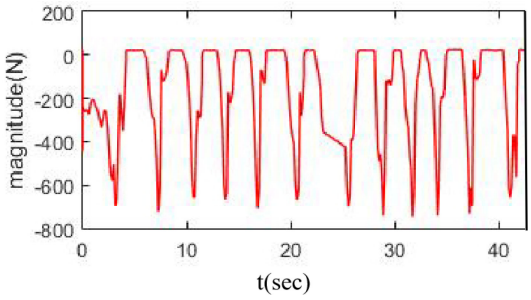

Fig. 12. Ground reactive force under level ground.

TABLE IV
TRAJECTORY TRACKING PERFORMANCE OF THREE SUBJECT IN CASE S4

Subject	MEAN(rad)	MSE(rad)
1	0.019	0.096
2	0.009	0.074
3	0.013	0.074

E. Case S4

1) Experiment: This case is to verify the performance of the proposed control method on the stairs ascent and descent to conduct the smooth and adaptive transitions between different terrain conditions, as shown in Fig. 13. There are five steps for the stairs ascent. Each step is about 12 cm high and 28 cm wide. The stairs descent have six steps. Each step is 10 cm high and 28 cm wide. When the subject walks up and down stairs, the stride length, height, and frequency of the leg prosthesis are conducted by the contralateral leg.

2) Results: The experimental results for the trajectory performance of different subjects are depicted in Figs. 14–15. It is observed that the desired trajectories are close to the measured ones in Fig. 14. The average deviation of tracking errors is presented in Table IV. As shown in Table IV, by regulating the parameters of leg prosthesis, the minimized MSE reduces to 0.060 rad, 0.046 rad, and 0.055 rad for subject 1, 2, and 3, respectively. Fig. 15 shows the ground reactive force during walking on stairs. The results in this experiment show that the tracking errors are small.

Fig. 13. Human-walking experiment under stairs.

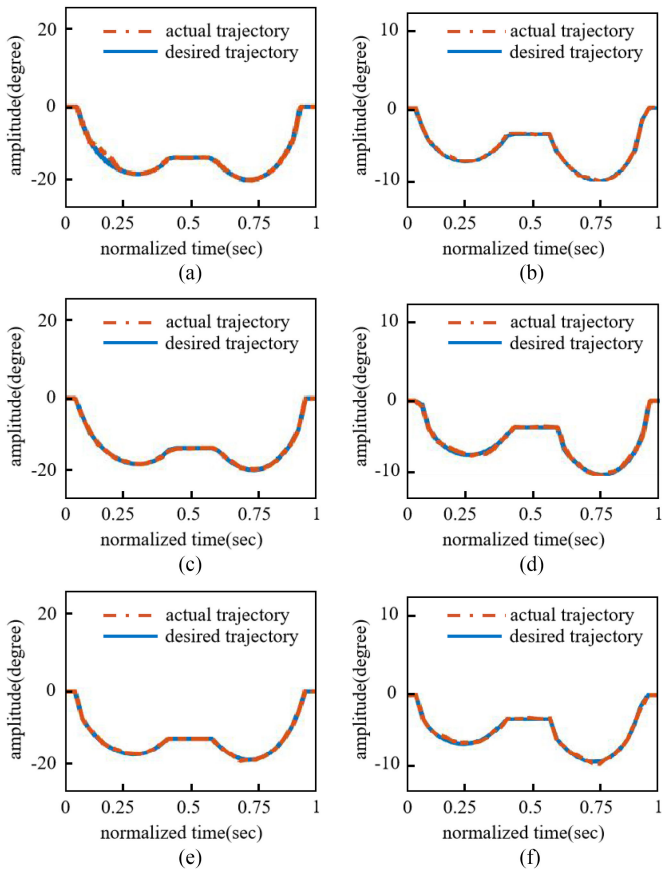

Fig. 14. Experimental results of three subjects. (a), (c), and (e) are the knee's tracking trajectories of subjects 1, 2, and 3, respectively. (b), (d), and (f) are the ankle's tracking trajectories of subjects 1, 2, and 3, respectively.

V. Discussion

This article aims to develop a method to help the subject with robotic leg prosthesis walk smoothly under various terrain conditions, without complex and empirical preconfigurations.

In fact, there are two IMU on the contralateral leg of subject to record the motion of the contralateral leg. By analyzing the recorded data, the initial values and the end values of each step of robotic leg prosthesis can be obtained. Then, the next touchdown state of leg prosthesis can be predicted by (9). The desired vertical and horizontal motion of the CoM can be calculated from (3) and (7). According to the inverse kinematics, the desired trajectory for the joints of the robotic leg prosthesis can be calculated. At last, the leg prosthesis restores the motion of the contralateral leg of subject.

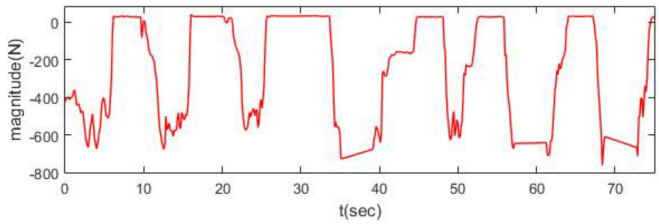

Fig. 15. Ground reactive force under stair ascent and descent.

The novelty of this proposed method includes the following. The walking of the leg prosthesis is encoded by polynomial splines using the initial position, the end position, and the time interval between steps, recorded by IMU mounted on the contralateral leg of subject. The walking trajectories can be reshaped according to different walking tasks, without complex preconfigurations and empirical tuning of the leg prosthesis. The proposed control method can smoothly achieve walking behaviors and diminish the overshoot of input torques caused by the large initial error at the beginning of the transient response, without exact knowledge of dynamics of leg prosthesis among different walking tasks.

The results of the experiments show the desired performance of the proposed control method. Without the knowledge of the terrain conditions, the smooth and adaptive transitions can be still realized for different walking tasks.

A limitation of the proposed approach is that we only tested three able-bodied subjects in the experiments. The other limitation is that it is necessary to instrument the contralateral leg of subject before conducting experiments.

VI. Conclusion

In this article, biologically inspired deadbeat control is proposed for the robotic leg prosthesis under different terrain conditions. As a result, the prosthesis can coordinate the movement of the subject and emulate the locomotion of contralateral leg more smoothly and adaptively. The merit of the proposed control method is that it works well without the preknowledge of the exact physical parameters. Finally, the experiments for different walking tasks have been conducted. The results show the effectiveness of the proposed control method.

References

[1] A. J. Young, A. M. Simon, and L. J. Hargrove, "A training method for locomotion mode prediction using powered lower limb prostheses," *IEEE Trans. Neural Syst. Rehabil. Eng.*, vol. 22, no. 3, pp. 671–667, May 2014.

[2] M. Zhang, W. Meng, T. C. Davies, Y. Zhang, and S. Xie, "A robot-driven computational model for estimating passive ankle torque with subject-specific adaptation," *IEEE Trans. Biomed. Eng.*, vol. 63, no. 4, pp. 814–821, 2016.
[3] A. H. Shultz, B. E. Lawson, and M. Goldfarb, "Running with a powered knee and ankle prosthesis," *IEEE Trans. Neural Syst. Rehabil. Eng.*, vol. 23, no. 3, pp. 403–412, May 2015.
[4] T. R. Clites *et al.*, "Proprioception from a neurally controlled lower-extremity prosthesis," *Sci. Translational Medicine*, vol. 10, no. 443, 2018, Art. no. eaap8373.
[5] R. Unal, S. Behrens, R. Carloni, E. Hekman, S. Stramigioli, and B. Koopman, "Conceptual design of a fully passive transfemoral prosthesis to facilitate energy-efficient gait," *IEEE Trans. Neural Syst. Rehabil. Eng.*, vol. 26, no. 12, pp. 2360–2366, Dec. 2018.
[6] J. D. Lee, L. M. Mooney, and E. J. Rouse, "Design and characterization of a quasi-passive pneumatic foot-ankle prosthesis," *IEEE Trans. Neural Syst. Rehabil. Eng.*, vol. 25, no. 7, pp. 823–831, Jul. 2017.
[7] K. Shamaei, P. C. Napolitano, and A. M. Dollar, "Design and functional evaluation of a quasi-passive compliant stance control knee anklefoot orthosis," *IEEE Trans. Neural Syst. Rehabil. Eng.*, vol. 22, no. 2, pp. 258–268, Mar. 2014.
[8] E. M. Glanzer and P. G. Adamczyk, "Design and validation of a semi-active variable stiffness foot prosthesis," *IEEE Trans. Neural Syst. Rehabil. Eng.*, vol. 26, no. 12, pp. 2351–2359, Dec. 2018.
[9] A. M. Simon *et al.*, "Configuring a powered knee and ankle prosthesis for transfemoral amputees within five specific ambulation modes," *PLoS One*, vol. 9, no. 6, 2014, Art. no. e99387.
[10] A. J. Young and L. J. Hargrove, "A classification method for user-independent intent recognition for transfemoral amputees using powered lower limb prostheses," *IEEE Trans. Neural Syst. Rehabil. Eng.*, vol. 24, no. 2, pp. 217–225, Feb. 2016.
[11] A. Pagel, R. Ranzani, R. Riener, and H. Vallery, "Bio-inspired adaptive control for active knee exoprosthetics," *IEEE Trans. Neural Syst. Rehabil. Eng.*, vol. 25, no. 12, pp. 2355–2364, Dec. 2017.
[12] A. H. Shultz, B. E. Lawson, and M. Goldfarb, "Variable cadence walking and ground adaptive standing with a powered ankle prosthesis," *IEEE Trans. Neural Syst. Rehabil. Eng.*, vol. 24, no. 4, pp. 495–505, Apr. 2016.
[13] A. M. Simon *et al.*"Delaying ambulation mode transition decisions improves accuracy of a flexible control system for powered knee-ankle prosthesis," *IEEE Trans. Neural Syst. Rehabil. Eng.*, vol. 25, no. 8, pp. 1164–1171, Aug. 2017.
[14] M. K. Shepherd, and E. J. Rouse, "The VSPA foot: A quasi-passive ankle-foot prosthesis with continuously variable stiffness," *IEEE Trans. Neural Syst. Rehabil. Eng.*, vol. 25, no. 12, pp. 2375–2386, Dec. 2017.
[15] S. Huang, J. P. Wensman, and D. P. Ferris, "Locomotor adaptation by transtibial amputees walking with an experimental powered prosthesis under continuous myoelectric control," *IEEE Trans. Neural Syst. Rehabil. Eng.*, vol. 24, no. 5, pp. 573–581, May 2016.
[16] N. Thatte and H. Geyer, "Toward balance recovery with leg prostheses using neuromuscular model control," *IEEE Trans. Biomed. Eng.*, vol. 63, no. 5, pp. 904–913, May 2016.
[17] Q. C. Ding, J. D. Han, and X. G. Zhao, "Continuous estimation of human multi-joint angles from sEMG using a state-space model," *IEEE Trans. Neural Syst. Rehabil. Eng.*, vol. 25, no. 9, pp. 1518–1528, Sep. 2017.
[18] N. Aghasadeghi, H. Zhao, L. J. Hargrove, A. D. Ames, E. J. Perreault, and T. Bretl, "Learning impedance controller parameters for lower-limb prostheses," in *Proc. IEEE/RSJ Int. Conf. Intell. Robots Syst.*, 2013, pp. 4268–4274.
[19] H. Huang, D. L. Crouch, M. Liu, G. S. Sawicki, and D. Wang, "A cyber expert system for auto-tuning powered prosthesis impedance control parameters," *Ann. Biomed. Eng.*, vol. 44, no. 5, pp. 1613–1624, 2016.
[20] J. Realmuto, G. Klute, and S. Devasia, "Preliminary investigation of symmetry learning control for powered ankle-foot prostheses," in *Proc. Wearable Robot. Assoc. Conf.*, 2019, pp. 40–45.
[21] S. Culver, H. Bartlett, A. Shultz, and M. Goldfarb, "A stair ascent and descent controller for a powered ankle prosthesis," *IEEE Trans. Neural Syst. Rehabil. Eng.*, vol. 26, no. 5, pp. 993–1002, May 2018.
[22] Y. Wen, J. Si, X. Gao, S. Huang, and H. H. Huang, "A new powered lower limb prosthesis control framework based on adaptive dynamic programming," *IEEE Trans. Neural Netw. Learn. Syst.*, vol. 28, no. 9, pp. 2215–2220, Sep. 2017.
[23] A. H. Shultz and M. Goldfarb, "A unified controller for walking on even and uneven terrain with a powered ankle prosthesis," *IEEE Trans. Neural Syst. Rehabil. Eng.*, vol. 26, no. 4, pp. 788–797, Apr. 2018.
[24] E. D. Ledoux and M. Goldfarb, "Control and evaluation of a powered transfemoral prosthesis for stair ascent," *IEEE Trans. Neural Syst. Rehabil. Eng.*, vol. 25, no. 7, pp. 917–924, Jul. 2017.
[25] G. Khademi, H. Mohammadi, H. Richter, and D. Simon, "Optimal mixed tracking/impedance control with application to transfemoral prostheses with energy regeneration," *IEEE Trans. Biomed. Eng.*, vol. 65, no. 4, pp. 894–910, Apr. 2018.
[26] M. Kim, T. J. Chen, T. Y. Chen, and S. H. Collins, "An anklefoot prosthesis emulator with control of plantarflexion and inversioneversion torque," *IEEE Trans. Robot.*, vol. 34, no. 5, pp. 1183–1194, Oct. 2018.
[27] M. Zhang, S. Xie, X. Li, G. Zhu, W. Meng, X. Huang, and A. Veale, "Adaptive patient-cooperative control of a compliant ankle rehabilitation robot (CARR) with enhanced training safety," *IEEE Trans. Ind. Electron.*, vol. 65, no. 2, pp. 1398–1407, 2018.
[28] D. Quintero, D. J. Villarreal, D. J. Lambert, S. Kapp, and R. D. Gregg, "Continuous-phase control of a powered knee ankle prosthesis: Subject experiments across speeds and inclines," *IEEE Trans. Robot.*, vol. 34, no. 3, pp. 686–701, Jun. 2018.
[29] J. Englsberger, P. Kozowski, C. Ott, and A. A. Schäffer, "Biologically inspired deadbeat control for running: From human analysis to humanoid control and back," *IEEE Trans. Robot.*, vol. 32, no. 4, pp. 854–867, Aug. 2016.
[30] N. P. Fey, A. M. Simon, A. J. Young, and L. J. Hargrove, "Controlling knee swing initiation and ankle plantarflexion with an active prosthesis on level and inclined surfaces at variable walking speeds," *IEEE J. Translational Eng. Health Medicine*, vol. 2, Jul. 2014, Art. no. 2100412.
[31] B. E. Lawson, B. Ruhe, A. Shultz, and M. Goldfarb, "A powered prosthetic intervention for bilateral transfemoral amputees," *IEEE Trans. Biomed. Eng.*, vol. 62, no. 4, pp. 1042–1050, Apr. 2015.
[32] A. E. Martin and R. D. Gregg, "Stable, robust hybrid zero dynamics control of powered lower-limb prostheses," *IEEE Trans. Autom. Control*, vol. 62, no. 8, pp. 3930–3942, Aug. 2017.
[33] M. Liu, D. Wang, and H. Huang, "Development of an environment-aware locomotion mode recognition system for powered lower limb prostheses," *IEEE Trans. Neural Syst. Rehabil. Eng.*, vol. 24, no. 4, pp. 434–443, Apr. 2016.
[34] D. L. Grimes, W. C. Flowers, and M. Donath, "Feasibility of an active control scheme for above knee prostheses," *J. Biomechanical Eng.-Trans. ASME*, vol. 99, no. 4, pp. 215–221, 1977.

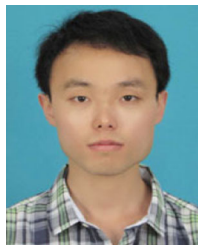

Ming Pi received the master's degree in automation from the Southwest University of Science and Technology, Sichuan, China, in 2014. He is currently working toward the Ph.D. degree in automation with the University of Science and Technology of China, Hefei, China.

His current research interests include the biped robot control and the robotic leg prostheses control.

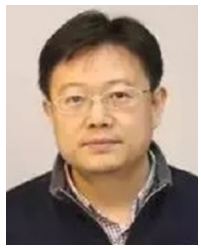

Zhijun Li (Senior Member, IEEE) received the Ph.D. degree in mechatronics, Shanghai Jiao Tong University, Shanghai, China, in 2002.

From 2003 to 2005, he was a Postdoctoral Fellow with the Department of Mechanical Engineering and Intelligent Systems, The University of Electro-Communications, Tokyo, Japan. From 2005 to 2006, he was a Research Fellow with the Department of Electrical and Computer Engineering, National University of Singapore, and Nanyang Technological University, Singapore. From 2017, he is a Professor with the Department of Automation, University of Science and Technology, Hefei, China. From 2019, he is the Vice Dean of School of Information Science and Technology, University of Science and Technology of China, China. His current research interests include wearable robotics, tele-operation systems, nonlinear control, neural network optimization, etc.

Dr. Li has been the Co-Chairs of IEEE SMC Technical Committee on Biomechatronics and Biorobotics Systems (B^2S), and IEEE RAS Technical Committee on Neuro-Robotics Systems since 2016. He is an Editor-at-large of *Journal of Intelligent and Robotic Systems*, and Associate Editors of several IEEE TRANSACTIONS.

Qinjian Li received the B.S. degree in automation from the Nanjing Institute of Technology, Nanjing, China, in 2015. He is currently working toward the Ph.D. degree in automation with the University of Science and Technology of China, Hefei, China.

His current research interests include design, simulation, and control of robotic leg prostheses.

Zhen Kan received the Ph.D. degree in mechanical and aerospace engineering from the University of Florida, Gainesville, FL, USA, in 2011.

He is a Professor with the Department of Automation, University of Science and Technology of China, Hefei, China. He was a Postdoctoral Research Fellow with the Air Force Research Laboratory, Eglin AFB, FL, USA, and the University of Florida REEF, Shalimar, FL, USA, from 2012 to 2016, and an Assistant Professor with the Department of Mechanical Engineering, University of Iowa, Iowa City, IA, USA. His current research interests include networked robotic systems, Lyapunov-based nonlinear control, graph theory, complex networks, and human-assisted estimation, planning, and decision making.

Prof. Kan is currently an Associate Editor with the Conference Editorial Board of the IEEE Control Systems Society and Technical Committee for several internationally recognized scientific and engineering conferences.

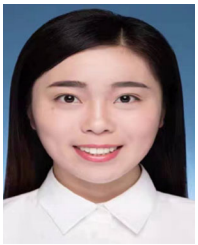

Cuichao Xu received the B.S. degree in vehicle engineering from the Hefei University of Technology, Hefei, China, in 2017. She is currently working toward the M.S. degree in control theory and control engineering with the University of Science and Technology of China, Hefei, China.

Her current research interests include mechanical design, simulation, and control.

Yu Kang (Senior Member, IEEE) received the Dr.Eng. degree in control theory and control engineering from the University of Science and Technology of China, Hefei, China, in 2005.

From 2005 to 2007, he was a Postdoctoral Fellow with the Academy of Mathematics and Systems Science, Chinese Academy of Sciences, Beijing, China. He is currently a Professor with the Department of Automation, and with the State Key Laboratory of Fire Science, and with the Institute of Advanced Technology, University of Science and Technology of China. His current research interests include adaptive/robust control, variable structure control, mobile manipulator, and Markovian jump systems.

Chun-Yi Su (Senior Member, IEEE) received the Ph.D. degree in control engineering from the South China University of Technology, Guangzhou, China, in 1990.

After a seven-year stint with the University of Victoria, he joined Concordia University in 1998. He has authored or coauthored more than 300 publications, which have appeared in journals, as book chapters and in conference proceedings. He conducts research in the application of automatic control theory to mechanical systems. He is particularly interested in control of systems involving hysteresis nonlinearities.

Dr. Su was an Associate Editor for the IEEE TRANSACTIONS ON AUTOMATIC CONTROL and IEEE TRANSACTIONS ON CONTROL SYSTEMS TECHNOLOGY, and *Journal of Control Theory and Applications*. He is on the Editorial Board of 14 journals, including IFAC *journals of Control Engineering Practice and Mechatronics*. He has also severed for many conferences as an organizing committee member, including General Co-Chair of the 2012 IEEE International Conference on Mechatronics and Automation, and Program Chair of the 2007 IEEE Conference on Control Applications.

Chenguang Yang (Senior Member, IEEE) received the B.Eng. degree in measurement and control from Northwestern Polytechnical University, Xi'an, China, in 2005, the Ph.D. degree in control engineering from the National University of Singapore, Singapore, in 2010, and postdoctoral training in human robotics from the Imperial College London, London, U.K.

He has been awarded EU Marie Curie International Incoming Fellowship, UK EPSRC UKRI Innovation Fellowship, and the Best Paper Award of the IEEE TRANSACTIONS ON ROBOTICS as well as over ten conference Best Paper Awards. His research interests include human robot interaction and intelligent system design.